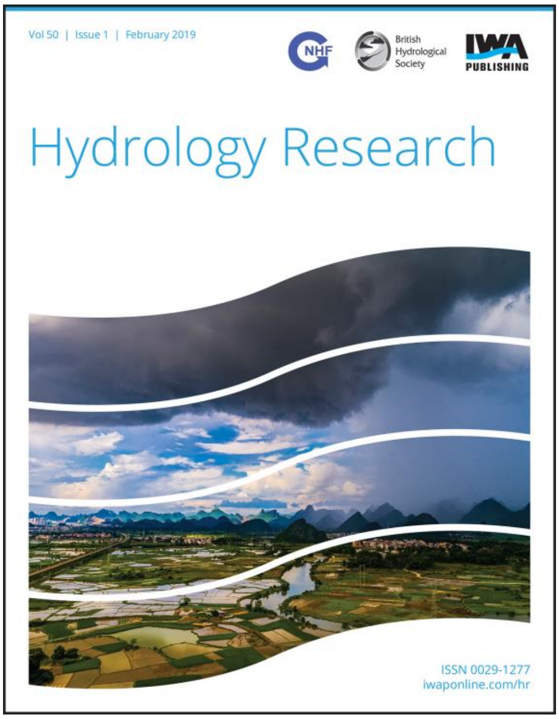
Vol 50 | Issue 1 | February 2019
NHF
British Hydrological Society
IWA PUBLISHING
Hydrology Research
ISSN 0029-1277
iwaponline.com/hr

Modelling soil detachment capacity by rill flow with hydraulic variables on a simulated steep loessial hillslope

Nan Shen, Zhanli Wang, Qingwei Zhang, Hao Chen and Bing Wu

ABSTRACT

Modelling soil detachment capacity by rill flow with hydraulic variables is essential to understanding the rill erosion process and developing physically based rill erosion models. A rill flume experiment with non-erodible flume bed and small soil samples was conducted. Seven flow discharges and six steep slope gradients were combined to produce various flow hydraulics. The soil detachment capacity increases with the increase in slope gradient and flow discharge. The critical slope gradients of 21.26 and 26.79% cause the detachment capacity to increase at a slow pace. The soil detachment capacity can be defined by a power function of flow discharges and slopes. The contribution rates of slope gradient and flow discharge to soil detachment capacity are 42 and 54%, respectively. The soil detachment capacity increases with shear stress, stream power and unit stream power; the increase rates of these parameters are greater under gentle slopes than steep slopes. Stream power is the superior hydrodynamic parameter describing soil detachment capacity. The linear model equation of stream power is stable and reliable, which can accurately predict soil detachment capacity by rill flow on steep loessial hillslopes. This study can help to sufficiently clarify the dynamic mechanism of soil detachment and accurately predict soil detachment capacity for steep loessial hillslopes.

Key words | flume experiment, hydraulic parameters, rill erosion, soil detachment capacity

Nan Shen
Zhanli Wang (corresponding author)
Qingwei Zhang
Hao Chen
State Key Laboratory of Soil Erosion and Dryland Farming on the Loess Plateau, Institute of Soil and Water Conservation,
Northwest A&F University,
Yangling, Shaanxi 712100,
China
E-mail: *zwang@nwsuaf.edu.cn*

Zhanli Wang
Bing Wu
State Key Laboratory of Soil Erosion and Dryland Farming on the Loess Plateau, Institute of Soil and Water Conservation,
Chinese Academy of Sciences and Ministry of Water Resources,
Yangling, Shaanxi 712100,
China

INTRODUCTION

The three sub-processes of rill erosion are soil detachment, transport and deposition of soil particles by erosive forces of rill flow. Soil detachment by rill flow is the initial phase of rill erosion, which provides a sediment source for runoff transport. Sediment load in rill flow increases with the downslope distance whilst the process of sediment transport continues (Nord & Esteves 2007; Chen *et al.* 2017). The increased sediment load causes a high energy expenditure for transporting sediment (Zhang *et al.* 2009b), a suppressed localized turbulence of runoff (Bennett *et al.* 2014), a shield soil bed (Merten *et al.* 2001) and thus a decreased soil detachment rate (Cochrane & Flanagan 1997; Lei *et al.* 2002). Soil detachment capacity by rill flow is the maximum soil detachment rate when no sediment exists in the rill flow (clear water), thereby indicating the maximum possibility of soil detachment by rill flow (Foster 1982; Nearing *et al.* 1991). Soil detachment capacity by rill flow is the key parameter for predicting rill erosion intensity. This parameter is widely introduced in the physical process-based soil erosion models, such as WEPP (Water Erosion Predict Project). Accurately modelling soil detachment capacity by rill flow is essential to understanding the rill erosion process, developing physically based rill erosion models and accurately predicting rill erosion intensity.

Soil detachment capacity is controlled primarily by flow hydraulics and soil properties (Mamo & Bubenzer 2001; Su *et al.* 2014; Chen *et al.* 2016; Liu *et al.* 2016). For a given soil, flow hydraulics control the process of soil detachment (Govers 1992; Zhang *et al.* 2003; Li *et al.* 2015). Slope gradient and flow discharge are important condition factors that determine the hydraulic properties of rill flow directly and are the most easily obtainable hydraulic variables.

doi: 10.2166/nh.2018.037

Modelling soil detachment capacity using slope gradient and flow discharge is practical and operable.

Nearing *et al.* (1991, 1997) studied the influence of soil and hydraulic parameters on the detachment of soil by shallow surface flow using a small soil sample in a hydraulic flume. The experimental results indicated that slope and flow depths were significant factors for detachment rates, and the soil detachment rate is more sensitive to slope than to flow depth (Nearing *et al.* 1997). The laboratory rainfall simulation experiment conducted by Zartl *et al.* (2001) confirmed the importance of slope for rill erosion. Chen *et al.* (2016) estimated the rill erosion process using the volume replacement method in eroded rills. The results showed that the cumulative eroded amounts linearly increased with increasing slope gradients and flow discharges; slope gradient serves as an important role in the overall erosion intensity.

However, Zhang *et al.* (2002) studied the soil detachment capacity by a flume experiment with constant roughness; the results indicated that flow discharge showed a stronger influence on the soil detachment rate compared with slope gradient. Xiao *et al.* (2017) performed an indoor concentrated flow scouring experiment with an erodible flume bed on steep loessial slopes to investigate soil detachment rates. The results showed a power function among soil detachment rate, flow discharge and slope gradient, and the soil detachment rate was more sensitive to discharge than to slope gradient. Zhang *et al.* (2008) developed a rare earth elements tracer method to quantify the rill erosion process. A linear relationship was determined to model the soil detachment rate by slope and flow discharges. The detachment rate was more affected by discharge than by slope gradients deduced from the relative magnitudes of their coefficients. The same results were found from the field simulation experiments on road surfaces conducted by Cao *et al.* (2011).

Flow shear stress, stream power and unit stream power are the commonly used hydrodynamic parameters which can reflect flow hydraulics from the perspective of force and energy. The exploration of the relationship between soil detachment capacity and hydrodynamic parameters and identification of the superior parameter that can accurately predict soil detachment capacity is significant for revealing the dynamic mechanism of soil detachment and developing a process-based rill erosion model.

Lyle & Smerdon (1965) first used a flume with a constant slope to investigate the relationship between the detachment rate and shear stress for a given soil and concluded that a unique relationship exists between them. Meyer & Wischmeier (1969) presented an erosion model under the slope condition of an average steepness of 8%; in this model, soil detachment by runoff is described by a function of shear stress. In the famous process-based soil erosion model WEPP, soil detachment capacity is also described by a linear function of the flow shear stress acting on the soil (Nearing *et al.* 1989). Franti *et al.* (1999) used shear stress for predicting soil detachment from the high-discharge concentrated flow. Furthermore, Gimenez & Govers (2002) studied soil detachment by concentrated flow on different beds and confirmed the good performance of the shear stress in the prediction of flow detachment. Cao *et al.* (2011) also confirmed that shear stress is the optimal estimator to predict the detachment rate. Wang *et al.* (2012) conducted laboratory experiments which showed that the detachment rate is linearly correlated with shear stress. However, erodibilities and critical shear stresses are different among the soil samples they used. The detachment capacity can be simulated by flow shear stress, cohesion and biological soil crusts coverage using a power function when soil samples are not identical (Liu *et al.* 2016).

Elliot & Laflen (1993) and Nearing (Nearing 1997; Nearing *et al.* 1999) showed that stream power is preferable to shear stress as a predictor for soil detachment and sediment yield. Zhang *et al.* (2002, 2003) performed a flume experiment which verified that stream power is the ultimate hydraulic parameter for predicting the detachment rate with a power function. Su *et al.* (2014) proposed that the detachment capacity can be predicted by stream power, clay content and organic matter content for different soil types. Xiao *et al.* (2017) conducted a concentrated flow scouring experiment with an erodible flume bed; the experiment results indicated that stream power is an optimal hydraulic parameter for describing soil detachment. However, Zhang *et al.* (2008) indicated that obvious superiority is not discovered when stream power is used to predict rill detachment. In addition, Nearing *et al.* (1997) proposed the calculation of the probabilistic model, which indicated that detachment is not a unique function of either shear stress or stream power.

In the physically based soil erosion models of EUROSEM and LISEM (De Roo *et al.* 1996; Misra & Rose 1996; Morgan *et al.* 1998), the unit stream power is applied as the hydraulic variable on which the rill transport capacity is predicted. Ali *et al.* (2013) established a unit stream power-based sediment transport function to predict soil erosion. However, Wang *et al.* (2016) investigated the correlation between soil detachment capacity and hydrodynamic parameters and concluded that the performance of unit stream power on detachment capacity prediction is very poor. So, unit stream power may be a good predictor for sediment transport but may not be a good predictor for soil detachment.

Limitations still exist and further studies are still required, although the relationships between soil detachment capacity/rate and hydraulic variables have been studied in the abovementioned literature. First, although slope and flow discharge were widely used to model soil detachment capacity, the main factor that influences soil detachment capacity is still unclear. The contributions of flow discharge and slope gradients to soil detachment capacity have not been quantified in terms of exact numbers. Second, it is uncertain which is the optimal hydrodynamic parameter among shear stress, stream power and unit stream power that can model soil detachment capacity accurately, and few experimental studies have been aimed specifically at rill flow detachment and the condition of steep loessial hillslopes. The hydraulic characteristics of overland flow and erosion process on steep and gentle slopes are different (Nearing *et al.* 1997, 1999; Liu *et al.* 2000; Zhang *et al.* 2009a). Severe erosion frequently occurs on steep slopes (Jiang *et al.* 2015), and loessial soil is a soil type which is easily eroded (Zhang *et al.* 2008; Gao *et al.* 2014). Therefore, it is necessary to study soil detachment by rill flow on steep loessial hillslopes. Third, the experiment conducted on non-erodible flume bed and minimal soil samples is a pure detachment capacity experiment which can ensure that the soil sample is detached by clear water to eliminate the potential effect of sediment load in the flow on measured net soil detachment rate. However, few studies have used non-erodible flume beds and small samples. Finally, the datasets of many studies have not been divided into two parts, namely, modelling and validation datasets, which is statistically inaccurate for developing a reliable soil erosion model.

Therefore, the rill flume experiment with a non-erodible flume bed and small soil samples under the condition of steep slope and loessial soil was applied in this study. The objectives of this study are: (1) to study the variation characteristics of soil detachment capacity with flow discharges and slopes; (2) to model soil detachment capacity using flow discharges and slope gradients and quantify the contributions of flow discharge and slope gradients to soil detachment capacity with percentage values; (3) to investigate the response of soil detachment capacity to hydrodynamic parameters (shear stress, stream power and unit stream power); and (4) to model soil detachment capacity using the three hydrodynamic parameters, thereby obtaining the optimal hydrodynamic model of soil detachment capacity. The results will provide a comprehensive and systematic study on the relation between soil detachment capacity and hydraulic variables, which is helpful in revealing the dynamic mechanism of soil detachment by rill flow and accurately predicting the intensity of rill erosion, especially for the condition of steep loessial hillslopes, on which serious erosion frequently occurs.

MATERIALS AND METHODS

Experimental devices and designs

The experimental soil was loessial soil sampled from Ansai county, which is located in the heartland of the Loess Plateau, China. Particle size distribution of the loessial soil was 36.58% sand (2–0.05 mm), 54.72% silt (0.05–0.002 mm) and 8.7% clay (<0.002 mm), which indicates that the experimental soil is sandy loam soil.

Soil detachment capacity and flow hydraulics were measured in a flume 4 m in length, 0.1 m in width and 0.1 m in depth. The slope gradient of the flume can be adjusted in the range of 8.75–70.02%, i.e. 5–35°. The experimental soil was thinly glued to the flume bed so that natural roughness was simulated and the flume bed can keep constant for all experiments (non-erodible bed). A chamber was built at the downstream end of the flume. A soil container ($0.1 \times 0.1 \times 0.05\ m^3$) filled with test soil was inserted in the chamber to measure soil detachment capacity. The flume bed and soil container were at the same level after the soil container was inserted in the chamber. Tap water was supplied to the upstream end of the flume by a pump, and the discharge of the water flow was controlled by a flowmeter. Figure 1 shows the experimental devices.

Six slopes (10.51, 15.84, 21.26, 26.79, 32.49 and 38.39%) were combined with seven unit flow discharges (1.11, 1.56, 2.00, 2.44, 2.89, 3.33 and 3.78×10^{-3} m^2 s^{-1}). Forty-two combinations were performed to test soil detachment capacity by rill flow; each combination was repeated once. Rates of the soil detachment capacity of the first test and the repetition for the 42 combinations were in the range of 0.67–1.69. The repetition test was close to the first test for each combination. The repeatability of the experiment was acceptable.

Measurements

Flow hydraulics

Flow surface velocity was measured by a dye method and flow depth was measured by an electric probe. Nine flow surface velocities and 18 flow depths were measured for each combination of slope and flow discharge. The flow surface velocities were multiplied with a correction factor of 0.8 to convert the flow surface velocity into the mean flow velocity (Emmett 1970; Li *et al.* 1996). The details of the flow hydraulics measurement can be found in Shen *et al.* (2017). The data of flow velocity and flow depth were shared in these two studies.

Soil detachment capacity by rill flow

The test soil was moistened to achieve a moisture content of 14%. The wet test soil was hierarchically packed into the soil container to a bulk density of 1.2 g cm^{-3}. Then the soil container was put in a box with water in it to saturate the soil. At this point, the soil sample was prepared. The prepared soil sample was inserted into the chamber and was covered by a sliding plate. The sliding plate covering the soil sample was removed after adjusting the flow discharge and slope, and the soil detachment process by flowing water commenced. A 2 cm scouring depth was applied for each combination in order to reduce errors (Zhang *et al.* 2002). The sliding plate was placed back on the soil sample to stop the detachment process once the detachment depth was achieved. The detachment time was recorded.

Calculation

Soil detachment capacity

The soil detachment capacity by rill flow (D_c, kg m^{-2} s^{-1}) was calculated by the following Equation (1):

$$D_c = \frac{W}{t \times A} \quad (1)$$

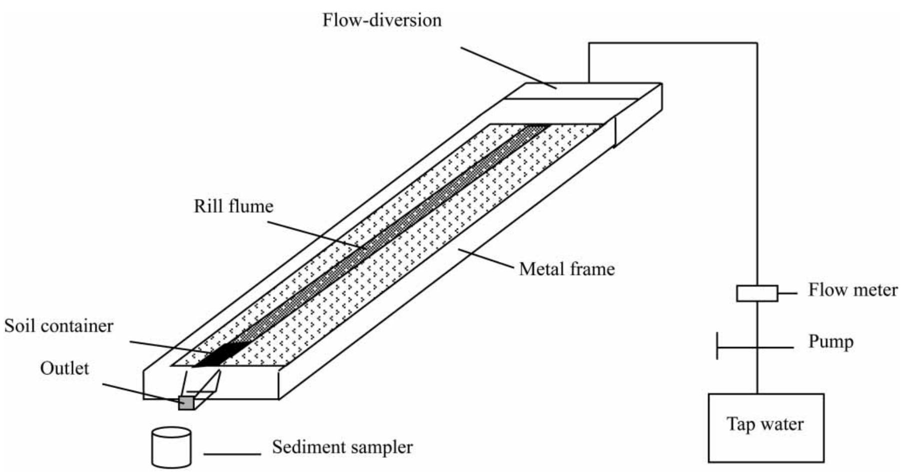

Figure 1 | Experimental devices.

where W is the weight of the detached soil (kg), t is detachment time (s), and A is the projected area of the soil sample (m^2).

Hydrodynamic parameters

Hydrodynamic parameters were calculated by Equations (2)–(4) (Bagnold 1966; Yang 1972; Nearing et al. 1991):

$$\tau = \rho g h S \tag{2}$$

$$\omega = \tau V \tag{3}$$

$$U = V \times S \tag{4}$$

where τ is shear stress (Pa), ρ is the water mass density (kg m^{-3}), g is the gravity constant (m s^{-2}), h is the flow depth (m), S is the slope gradient (m m^{-1} or %), ω is stream power (W m^{-2}), U is unit stream power (m s^{-1}) and V is the flow velocity (m s^{-1}).

Contribution rate

The contribution rate of factor i to the dependent variable, P_i, was calculated using Equation (5) (Huoluo 1983; Shen et al. 2017):

$$P_i = R^2 \frac{\beta_i^2}{\sum_{i=1}^{n} \beta_i^2} \times 100\% \tag{5}$$

where β_i is the standardized regression coefficient of factor i; R^2 is the determination coefficient of the multiple regression equation.

Data partition

A total of 42 datasets were obtained from the flume experiment. The 42 datasets were divided into two parts: 21 datasets were used as the modelling datasets to establish the model equations of soil detachment capacity by rill flow and the other 21 datasets were used as the verification datasets for evaluating the performances of the established model equations. The relative error (*RE*, %), mean absolute error (*MAE*, %), root mean square error (*RMSE*), determination coefficient (R^2) and Nash–Sutcliffe model efficiency (*NSE*) were used as statistical parameters to evaluate the performance of the equations (Nash & Sutcliffe 1970; Zhang et al. 2009b; Trenouth & Gharabaghi 2015; Thompson et al. 2016).

RESULTS AND DISCUSSION

Effect of flow discharge and slope gradient on soil detachment capacity by rill flow

The effect of slope gradient on soil detachment capacity by rill flow is illustrated in Figure 2. In this figure, the soil detachment capacity increased with the increase in slope gradients. The maximum rate of increase is obtained when the slope gradients reach 21.26% (Figure 2(a)–2(d) and 2(f)) and 26.79% (Figure 2(e) and 2(g)). The rate of increase was elevated with the increase in slope gradient when the slope gradients were gentler than 21.26 and 26.79%. The rate of increase decreased with slope gradients, or fluctuated irregularly with slope gradients (remained smaller than the increase rate of 21.26 and 26.79%) when the slope gradients were steeper than 21.26 and 26.79%. Thus, the two slope gradients of 21.26 and 26.79% may be the critical slope gradients, over which the soil detachment capacity began to increase at a slower pace than the maximum increase rate of the critical slope. The range of slope gradient in this study is recorded from 10.51 to 38.39%. Slope gradients that are steeper than 38.39% must be applied in future studies to further investigate the critical slope gradients and identify if one, or more than one, critical value is present.

The effect of flow discharges on soil detachment capacity by rill flow is depicted in Figure 3. In this figure, the soil detachment capacity increased with the increase in flow discharges. For the three relatively gentle slopes (Figure 3(a)–3(c)), the maximum rate of increase is obtained when the flow discharge is 0.00156 $m^2 s^{-1}$; for the three relatively steep slopes (Figure 3(d)–3(f)), the maximum rate of increase is obtained when the flow discharge is 0.00378 $m^2 s^{-1}$ (Figure 3(d)) and 0.00289 $m^2 s^{-1}$ (Figure 3(e) and 3(f)). Therefore, the variation features of soil detachment capacity with flow

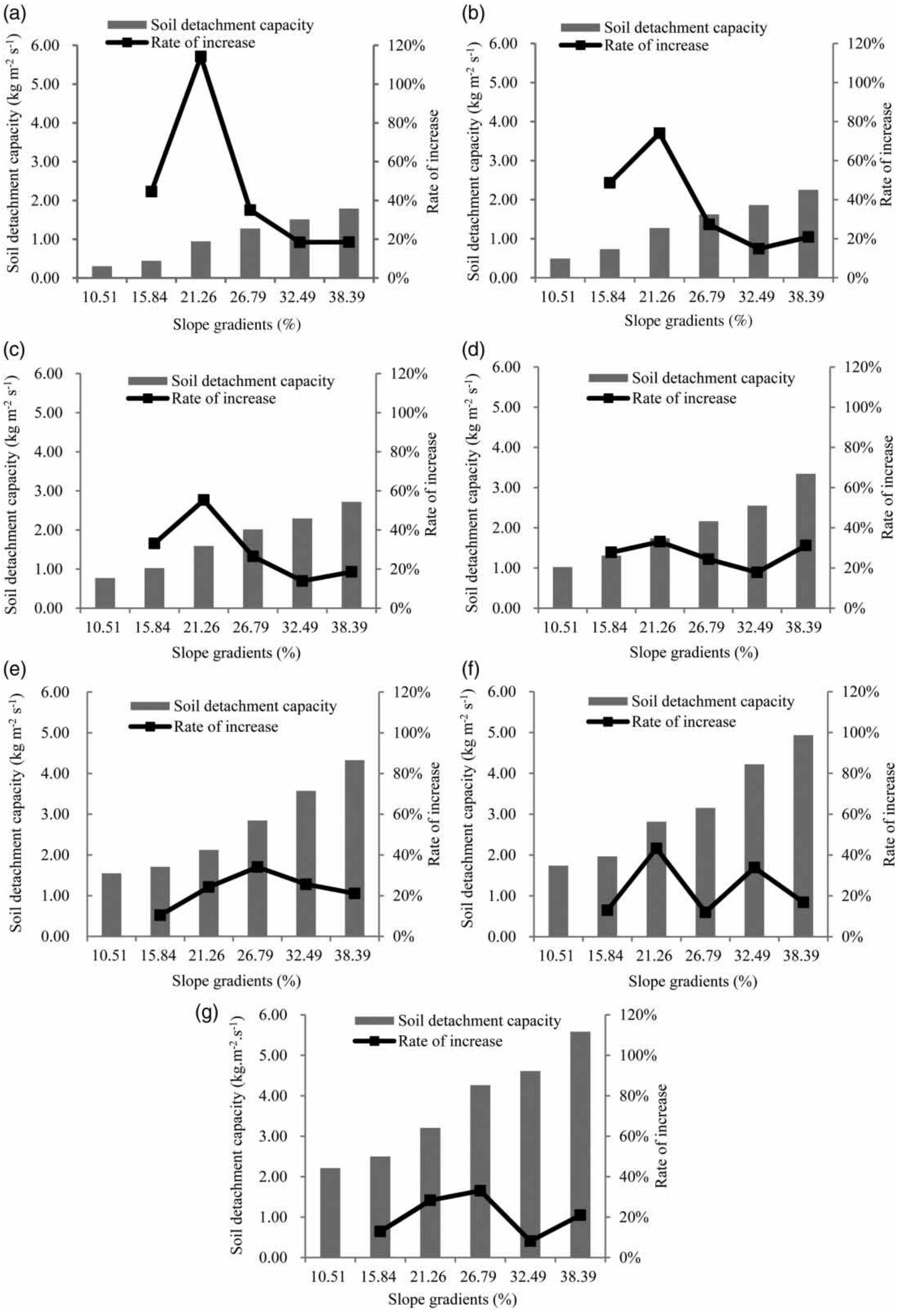

Figure 2 | Effect of slope gradients on soil detachment capacity by rill flow; (a), (b), (c), (d), (e), (f) and (g) are the seven different unit flow discharges: 0.00111, 0.00156, 0.00200, 0.00244, 0.00289, 0.00333 and 0.00378 m^2 s^{-1}.

discharges are different between gentle and steep slopes. However, the relationship where the soil detachment capacity increases with the increase in flow discharges is constant for all slopes. Ultimately, slope gradients and flow discharges are the positive factors that determine soil detachment capacity by rill flow.

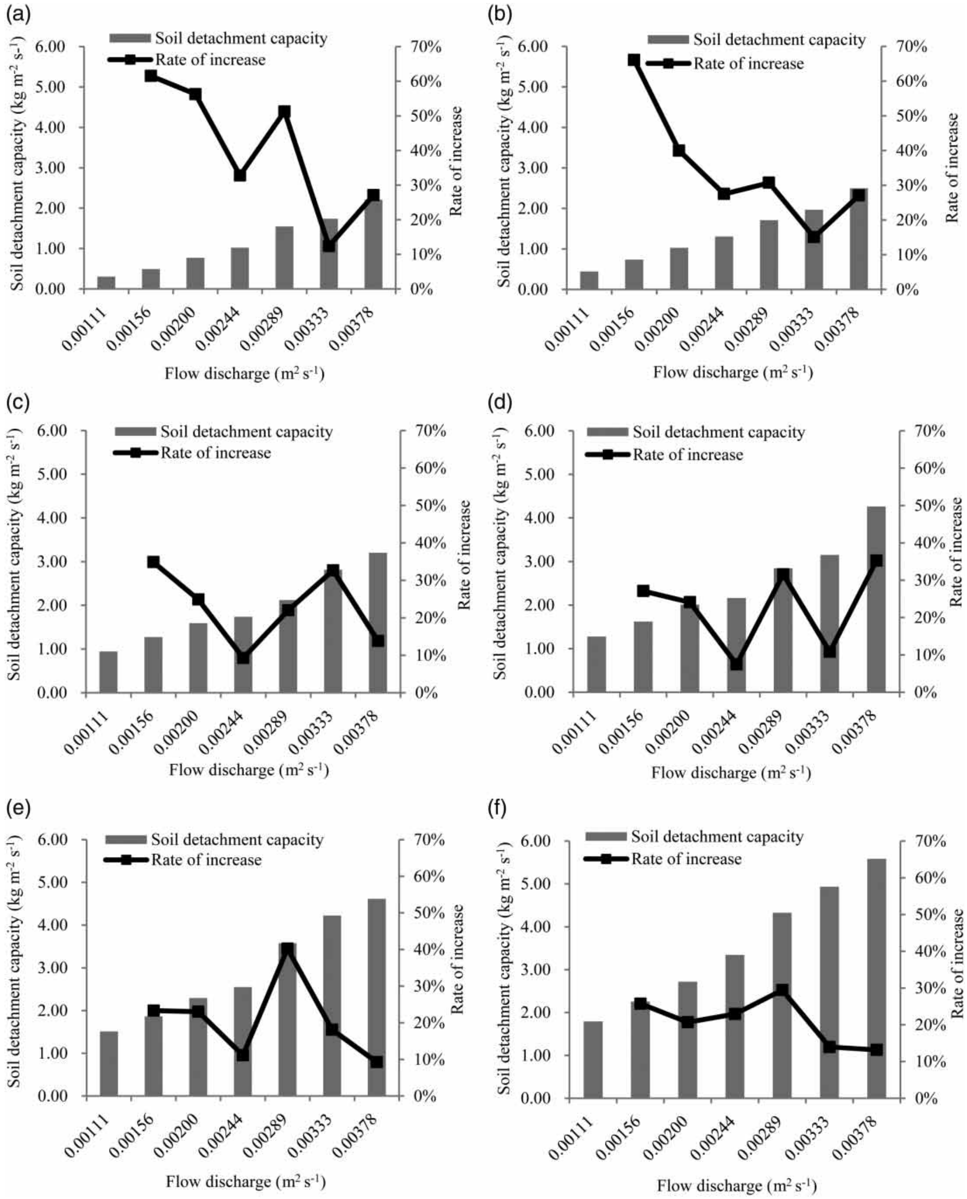

Figure 3 | Effect of flow discharge on soil detachment capacity by rill flow; (a), (b), (c), (d), (e) and (f) are the six slope gradients: 10.51, 15.84, 21.26, 26.79, 32.49 and 38.39%.

Modelling soil detachment capacity by rill flow using flow discharge and slope

The modelling soil detachment capacity using slope gradient and flow discharge is practical and operable because the two hydraulic condition factors are easily obtainable. A multiple nonlinear regression analysis based on the 21 sets of modelling data was applied to establish the relationship of soil detachment capacity with flow discharge and slope gradient. Slope gradient and flow discharge were used as the dependent variables, respectively, and soil detachment capacity by rill flow (D_c, kg·m^{-2}·s^{-1}) was used as the independent variable. The regression relationship is expressed as follows:

$$D_c = 76.5904\, S^{1.0148} Q^{1.1224} \tag{6}$$

$(R^2 = 0.9531;\ P < 0.001,\ n = 21)$

where S is slope gradient (%) and Q is the unit flow discharge ($m^2\ s^{-1}$).

Soil detachment capacity can be defined by a power function of flow discharges and slope gradients. The R^2 was at 0.9531, $P < 0.001$. Equation (6) was statistically significant, and soil detachment capacity by rill flow is determined by slopes and flow discharges collectively.

The contribution rate of each factor to the soil detachment capacity by rill flow must be identified to enhance the understanding of the process of soil detachment. The contribution rates of slope gradients and flow discharge to soil detachment capacity by rill flow were calculated by Equation (5), correspondingly, and the results are depicted in Figure 4. The contribution rate of slope gradient to soil detachment capacity was 42%, and the contribution rate of flow discharge to soil detachment capacity was 54%, thereby indicating that the influence of flow discharge on soil detachment capacity is higher than the influence of slope gradient. Flow discharge is the larger factor that influences the process of soil detachment, which is consistent with the results of Xiao *et al.* (2017) and Zhang *et al.* (2002, 2008). The adoption of water conservation measures to increase water infiltration and reduce surface runoff can decrease flow discharge and thus reduce rill erosion intensity (Liu *et al.* 2015). In addition, the contribution to soil detachment capacity is only 12.25% lower in slope gradients than in flow discharges; thus, the factor of slope gradients should also be highlighted.

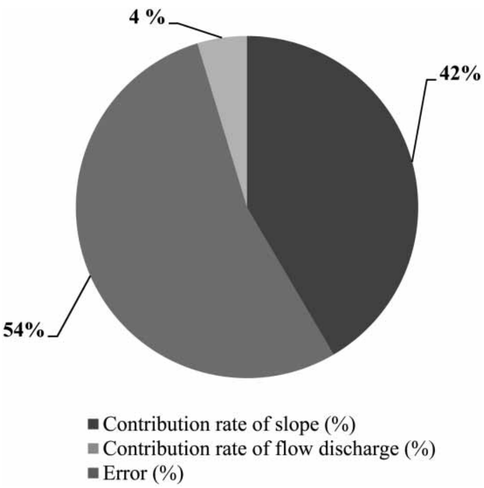

Figure 4 | Contribution rates of slope gradient and flow discharge to soil detachment capacity by rill flow.

The verification datasets were used to verify the performance of Equation (6), and the verification results are presented in Table 1 and Figure 5. The R^2 and NSE were 0.9690 and 0.9564, correspondingly. The RE between the predicted and measured soil detachment rates ranged from −38.5373 to 20.5039%; the MAE was 9.6862%, and $RMSE$ was 0.1381. Therefore, the prediction errors of Equation (6) were acceptable, and the predictive accuracy of Equation (6) was high. Figure 5 displays the predicted value calculated by using Equation (6) and the measured value obtained by the experiment. The data points were distributed near the 1:1 line; the predicted values approximate the measured values well. Therefore, Equation (6) satisfactorily predicts the soil detachment rate by rill flow. Equation (6) is a stable and reliable model equation that can accurately predict the soil detachment capacity using slope gradient and flow discharges. Soil detachment capacity is controlled primarily by flow hydraulics and soil properties (Mamo & Bubenzer 2001; Su *et al.* 2014; Chen *et al.* 2016; Liu *et al.* 2016). The relationship between soil detachment capacity and the hydraulic variables slope gradient and flow discharge was investigated. However, soil properties, such as soil types, soil mechanical composition, initial soil moisture

Table 1 | Statistics between measured and predicted soil detachment capacity using the established model equation of soil detachment capacity by rill flow for the verification datasets

Equation	R^2	*NSE*	*RE* (%)	*MAE* (%)	*RMSE*	*n*
$D_c = 76.5904\ S^{1.0148}Q^{1.1224}$ (6)	0.9690	0.9564	−38.5373–20.5039	9.6862	0.1381	21
$D_c = 0.5534\ (\tau - 2.3123)$ (7)	0.8682	0.8669	−32.6061–43.8264	16.7757	0.2413	21
$D_c = 0.4211\ (\omega - 0.6891)$ (8)	0.9466	0.9431	−27.2453–23.5370	9.6607	0.1578	21
$Dc = 10.582(U - 0.0181)$ (9)	0.6463	0.5904	−85.5218–50.9887	28.9023	0.4233	21

D_c is soil detachment capacity by rill flow (kg $m^{-2}\ s^{-1}$); S is slope gradient (%); Q is unit flow discharge ($m^2\ s^{-1}$); τ is shear stress (Pa); ω is stream power (W m^{-2}); U is unit stream power ($m^2\ s^{-1}$); *NSE* is Nash–Sutcliffe model efficiency; *RE* is relative error (%); *MAE* is mean absolute error (%); *RMSE* is root mean square error; *n* is number of datasets.

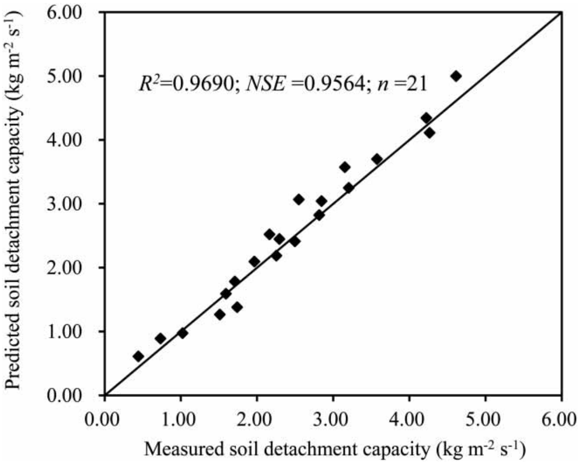

Figure 5 | Measured vs. predicted soil detachment capacity for the validation datasets using the model: $D_c = 76.5904S^{1.0148}Q^{1.1224}$.

conditions, soil bulk density, and vegetation growing in the soil, etc., are important factors that could influence the rill erosion process but were not investigated in this laboratory study.

Response of soil detachment capacity by rill flow to hydrodynamic parameters

The response of soil detachment capacity to the hydrodynamic parameters (shear stress, stream power and unit stream power) are demonstrated in Figure 6, in which Figure 6(a)–6(c) show the response at six slope gradients, while Figure 6(d)–6(f) show the response at seven flow discharges. Soil detachment capacity increased with the rising shear stress, stream power and unit stream power (Figure 6). The increase rate was higher in gentle slopes than in steep slopes (Figure 6(a)–6(c)), thereby indicating that the response of soil detachment capacity to the hydraulic parameters is more robust on gentle slopes than on steep slopes. This result corroborated the conclusions of Zhang *et al.* (2002) and Nearing *et al.* (1991), in which the relationship between the soil detachment rate and the hydraulic parameter varies with slope gradient. Further study needs to be carried out to investigate the adjustment factor of slope gradient to improve the accuracy of the modelling of the soil detachment capacity. The increase in rates of soil detachment capacity with the hydraulic parameters was nearly the same for the seven flow discharges (Figure 6(d)–6(f)). The response of soil detachment capacity to the hydraulic parameters is constant among the different flow discharges.

Modelling soil detachment capacity by rill flow using the hydrodynamic parameters

The relationship between soil detachment capacity and shear stress was analyzed based on the 21 modelling datasets. In Figure 7(a), the soil detachment capacity was increased with the increase in the shear stress. The regression analysis was performed for the modelling datasets to establish the relationship between soil detachment capacity (D_c, kg·m^{-2}·s^{-1}) and flow shear stress (τ, Pa). Below is the regression relationship:

$$D_c = 0.5534\,(\tau - 2.3123) \tag{7}$$

$(R^2 = 0.9068, P < 0.001, n = 21)$

Equation (7) shows that the soil detachment capacity can be defined by a linear function of shear stress. The R^2 was recorded at 0.9068, $P < 0.001$. Equation (7) is statistically significant, and the linear relationship summarized in Equation (7) between soil detachment capacity and shear stress indicated that rill erodibility (K_r) is 0.5534 s m^{-1} and critical shear stress (τ_c) is 2.3 Pa. The rill erodibility (K_r) of 0.5534 s m^{-1} in this study is nearly twice the values reported by Zhang *et al.* (2002); this value may be due to the large difference in soil mechanical composition. The loessial soil in this study consisted of 8.7% clay and 36.58% sand, but the soil used by Zhang *et al.* (2002) contained 23.6% clay and 16.8% sand. The low clay content and high sand content of loessial soil make it easy to be eroded. The critical shear stress (τ_c) of 2.3 Pa indicated that the soil detachment capacity by rill flow was generated only when the flow shear stress exceeded 2.3 Pa for the test loessial soil. The critical shear stress of this study is smaller than the values reported by Wang *et al.* (2012) and Zhang *et al.* (2002) but within the range of the values reported by Liu *et al.* (2016) and Laflen *et al.* (1991).

In Figure 7(b), the soil detachment capacity increased with the increasing stream power. The regression analysis

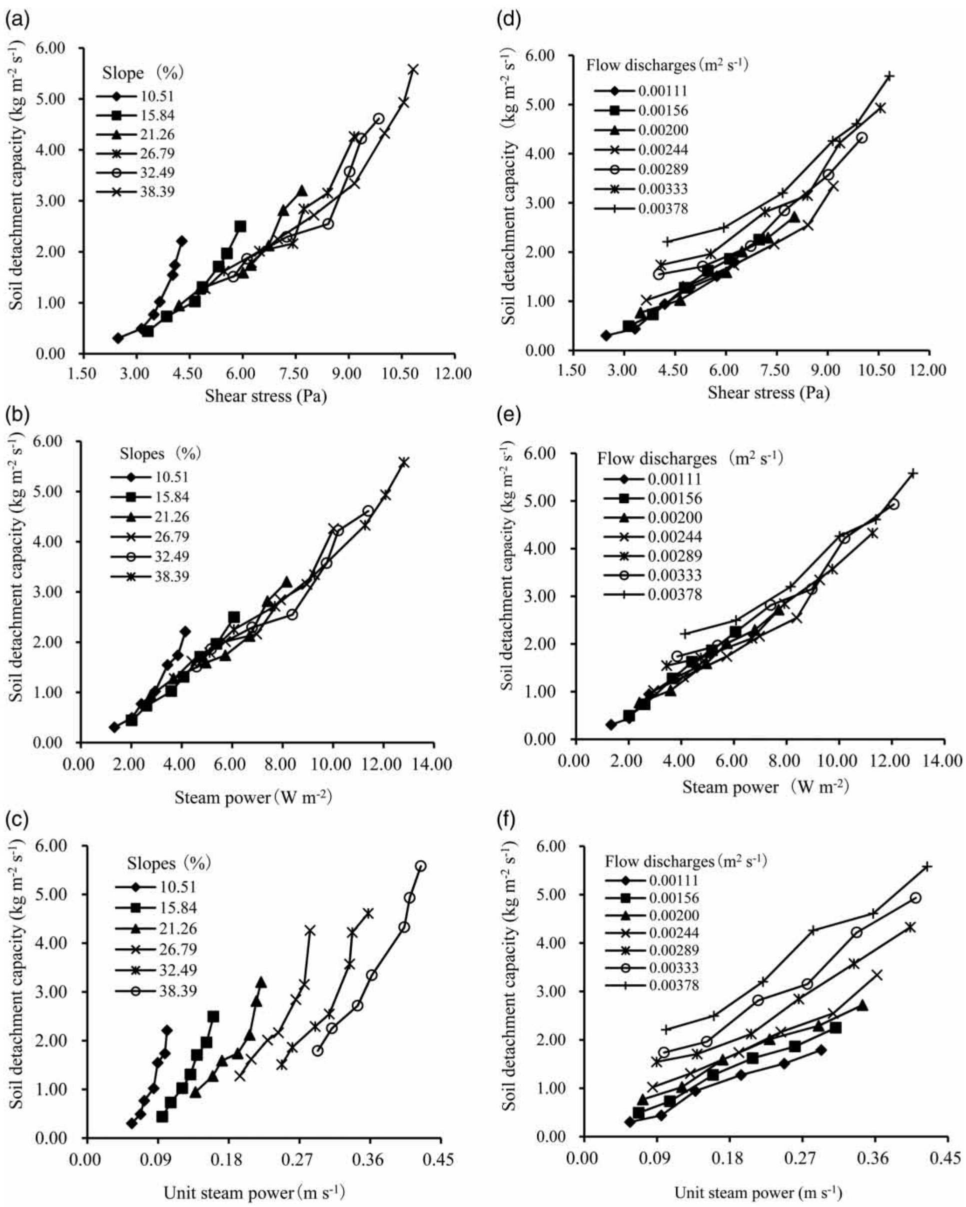

Figure 6 | Response of soil detachment capacity to hydrodynamic parameters at different slopes and flow discharges.

of the modelling datasets showed that the best-fitted relationship between soil detachment capacity and stream power (ω, W m^{-2}) is a linear function:

$$D_c = 0.4211(\omega - 0.6891) \quad (8)$$

$$(R^2 = 0.9623, P < 0.001, n = 21)$$

Equation (8) shows that the soil detachment capacity can be defined by a linear function of stream power. The R^2 was recorded at 0.9623, $P < 0.001$. Equation (8) is statistically significant. The horizontal intercept of the linear regression equation indicates that soil particles can be detached from the soil body only when the stream power exceeds almost 0.69 W m^{-2}; that is, 0.69 W m^{-2} is the critical stream power. Su *et al.* (2014) and Xiao *et al.* (2017) modelled the soil detachment capacity by a power function of the stream power, in which the critical stream power cannot be obtained. A

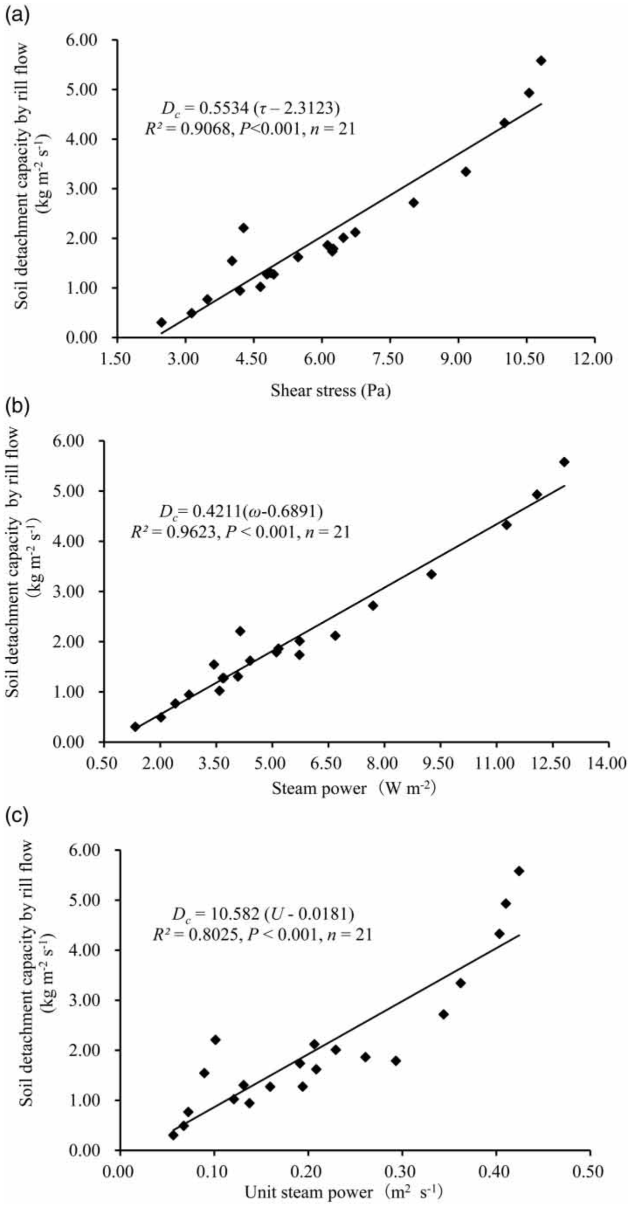

Figure 7 | Relationship between soil detachment capacity by rill flow and hydrodynamic parameters for the modelling datasets.

linear function can present more physical significance in comparison to a power function, which is helpful in developing a physically process-based soil erosion model.

For the unit stream power (U, $m^2\,s^{-1}$), the soil detachment capacity increased with the increase in the unit stream power (Figure 7(c)), and a simple linear function was established:

$$D_c = 10.582\,(U - 0.0181) \tag{9}$$

$$(R^2 = 0.8025, P < 0.001, n = 21)$$

Equation (9) shows that the soil detachment capacity can be described by a linear function of stream power. The R^2 was at 0.8025, $P < 0.001$. Equation (9) is statistically significant. The intercept of the regression equation indicates that detachment was only generated when the unit stream power exceeded 0.018 $m^2\,s^{-1}$.

The verification datasets were used to verify the performance of Equations (7)–(9), and the verification results are presented in Table 1 and Figure 8. Based on the statistical parameters R^2, *NSE*, *RE* (%), *MAE* (%) and *RSME* summarized in Table 1, the predictive accuracy of the three equations can be ranked in the order of stream power Equation (8) > shear stress Equation (7) > unit stream power Equation (9); that is, stream power is the optimal hydraulic parameter that demonstrates the highest predictive accuracy for soil detachment capacity by rill flow. Figure 8 displays the predicted value calculated by Equations (7)–(9) and the measured value obtained by the experiment for the validation datasets. As Figure 8(a) and 8(b) show, the predicted values calculated by shear stress Equation (7) and steam power Equation (8) approximate the measured values well, and the steam power equation performed slightly better than the shear stress equation. The data points were distributed relatively scattered around the 1:1 line when using unit stream power Equation (9). The predicted values calculated by the unit stream power equation are distinct from the measured values; thus, the performance of the unit stream power equation was unsatisfactory. In summary, stream power Equation (8) satisfactorily predicts the soil detachment rate by rill flow.

The above validation demonstrates that Equation (8) is a stable and reliable model equation that can predict soil detachment capacity by rill flow on steep loessial hillslopes accurately. In addition, stream power exhibited superior performance in modelling the soil detachment capacity compared with shear stress and unit stream power; stream power is the source of power for the process

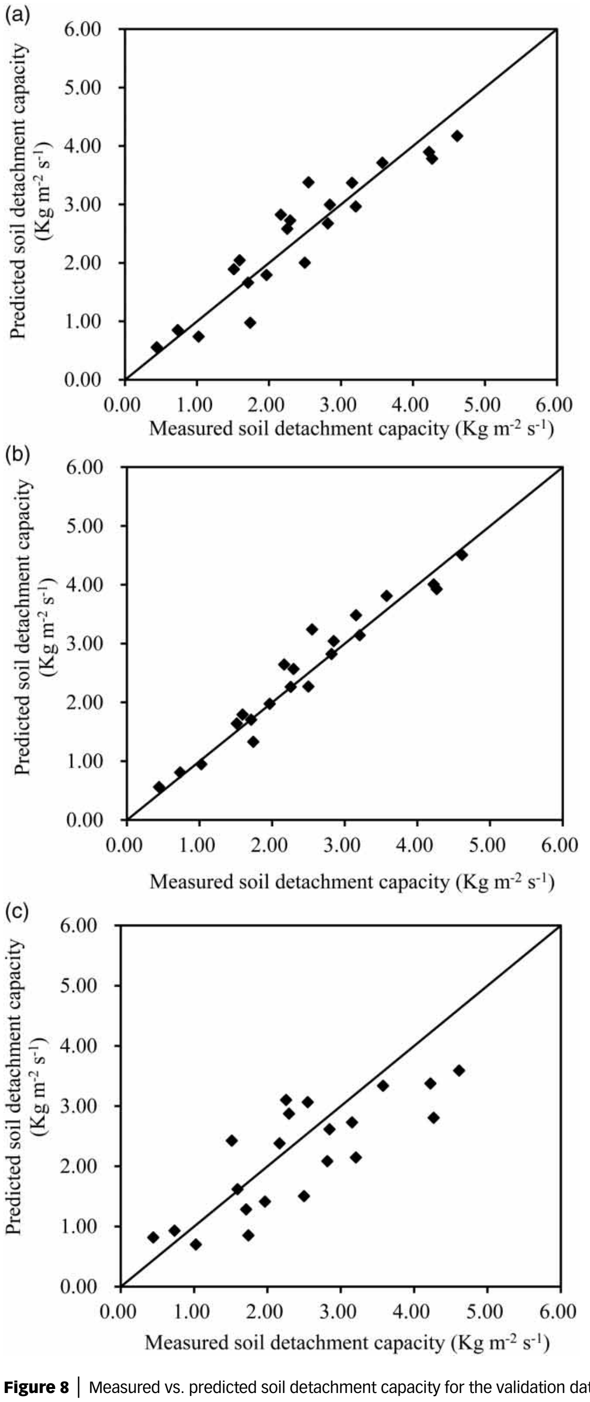

Figure 8 | Measured vs. predicted soil detachment capacity for the validation data (a), (b) and (c) mean using the model: $D_c = 0.5534\ (\tau–2.3123)$ (7), $D_c = 0.4211\ (\omega–0.6891)$ (8), and $D_c = 10.582\ (U–0.0181)$ (9).

of soil detachment. The current result is consistent with the conclusions proposed by Elliot & Laflen (1993), Nearing *et al.* (1999), Zhang *et al.* (2003), Li *et al.* (2015), Su *et al.* (2014) and Xiao *et al.* (2017), although the experimental conditions were different. The difference in experimental conditions only led to the differences in coefficients and forms of the equation but do not change the results that stream power is the optimal parameter for modelling soil detachment capacity.

CONCLUSIONS

This study modelled the soil detachment capacity by rill flow with hydraulic variables through a rill flume experiment at various flow discharges and steep slope gradients using loessial soil as the test material. The soil detachment capacity by rill flow increased with the increase in slope gradient and flow discharge. The rate of increase indicated that the slope gradients of 21.26 and 26.79% may be the critical slope gradients in which the soil detachment capacity begins to increase at a slow pace. Soil detachment capacity can be modelled by a power function of flow discharges and slopes, and flow discharge has a slightly greater contribution than slope gradient to soil detachment capacity. The contribution rate of slope gradient to soil detachment capacity was 42%, and the contribution rate of flow discharge was 54%. Soil detachment capacity increased with the three hydrodynamic parameters (shear stress, stream power and unit stream power). The rate of increase is greater under gentle slopes than steep slopes. The soil detachment capacity can be modelled by the linear functions of shear stress, stream power and unit stream power; stream power is the optimal hydraulic parameter in terms of soil detachment capacity among the three hydrodynamic parameters. The linear model equation of stream power is stable and reliable and can predict the soil detachment capacity by rill flow on steep loessial hillslopes accurately. This study helps in improving our understanding of the relationship between hydraulic variables and soil detachment capacity, revealing the dynamic mechanism of soil detachment and accurately predicting the soil detachment capacity for steep loessial hillslopes. This study only studied one type of soil, and the empirical equations developed may not work for other soil types. Soil types, vegetation, soil mechanical composition, initial soil moisture conditions, soil bulk density, and soil frost-heave are important field condition factors that could influence the rill erosion process but were not investigated in this laboratory study.

ACKNOWLEDGEMENTS

Financial support for this research was provided by the National Natural Science Foundation of China funded project (41471230; 41830758; 41601282; 41171227); the National Key Research and Development Program of China (2016YFC0402401; 2017YFD0800502); Special-Funds of Scientific Research Programs of State Key Laboratory of Soil Erosion and Dryland Farming on the Loess Plateau (A314021403-C2).

REFERENCES

Ali, M., Seeger, M., Sterk, G. & Moore, D. 2013 A unit stream power based sediment transport function for overland flow. *Catena* **101**, 197–204.
Bagnold, R. A. 1966 An approach to the sediment transport problem from general physics. *US Geol. Surv. Prof. Pap.* **422** (1), 22–37.
Bennett, S. J., Hou, Y. T. & Atkinson, J. F. 2014 Turbulence suppression by suspended sediment within a geophysical flow. *Environ. Fluid Mech.* **14** (4), 771–794.
Cao, L. X., Zhang, K. L., Dai, H. L. & Guo, Z. L. 2011 Modeling soil detachment on unpaved road surfaces on the Loess Plateau. *Trans. ASABE* **54** (4), 1377–1384.
Chen, X. Y., Zha, Y., Mi, H. X. & Mo, B. 2016 Estimating rill erosion process from eroded morphology in flume experiments by volume replacement method. *Catena* **136**, 135–140.
Chen, X. Y., Huang, Y. H., Zhao, Y., Mo, B., Mi, H. X. & Huang, C. H. 2017 Analytical method for determining rill detachment rate of purple soil as compared with that of loess soil. *J. Hydrol.* **549**, 236–243.
Cochrane, T. A. & Flanagan, D. C. 1997 Detachment in a simulated rill. *Trans. ASAE* **40** (1), 111–119.
De Roo, A. P. J., Wesseling, C. G. & Ritsema, C. J. 1996 LISEM: a single-event physically based hydrological and soil erosion model for drainage basins. 1. Theory, input and output. *Hydrol. Process.* **10** (8), 1107–1117.
Elliot, W. J. & Laflen, J. M. 1993 A process-based rill erosion model. *Trans. ASAE* **36** (1), 65–72.
Emmett, W. W. 1970 *The Hydraulics of Overland Flow on Hillslopes*. US Geol. Surv. Prof. Pap. A21. United States Department of the Interior, Washington, DC.
Foster, G. R. 1982 Modeling the erosion process. In: *Hydrologic Modeling of Small Watersheds* (C. T. Haan ed.). ASAE, Monogr. no. 5. ASAE, St. Joseph, MI, pp. 296–380.
Franti, T. G., Laflen, J. M. & Watson, D. A. 1999 Predicting soil detachment from high-discharge concentrated flow. *Trans. ASAE* **42** (2), 329–335.
Gao, P., Geissen, V., Temme, A. J. A. M., Ritsema, C. J., Mu, X. & Wang, F. 2014 A wavelet analysis of the relationship between loess plateau erosion and sunspots. *Geoderma* **213** (1), 453–459.
Gimenez, R. & Govers, G. 2002 Flow detachment by concentrated flow on smooth and irregular beds. *Soil Sci. Soc. Am. J.* **66** (5), 1475–1483.
Govers, G. 1992 Relationship between discharge, velocity and flow area for rills eroding loose, nonlayered materials. *Earth Surf. Process. Landf.* **17** (5), 515–528.
Huoluo, H. N. 1983 *The Prediction of Agricultural Production Effect*. Translated by Tan, J. W. & Liu, T. F. Agriculture Press, Beijing.
Jiang, L. G., Yao, Z. J., Liu, Z. F., Wu, S. S., Wang, R. & Wang, L. 2015 Estimation of soil erosion in some sections of Lower Jinsha River based on RUSLE. *Nat. Hazards* **76** (3), 1831–1847.
Laflen, J. M., Elliot, W. J., Simanton, J. R., Holzhey, C. S. & Kohl, K. D. 1991 WEPP: soil erodibility experiments for rangeland and cropland soils. *J. Soil Water Conserv.* **46** (1), 39–44.
Lei, T. W., Zhang, Q. W., Zhao, J., Xia, W. S. & Pan, Y. H. 2002 Soil detachment rates for sediment loaded flow in rills. *Trans. ASAE* **45** (6), 1897–1903.
Li, G., Abrahams, A. D. & Atkinson, J. F. 1996 Correction factors in the determination of mean velocity of overland flow. *Earth Surf. Process. Landf.* **21** (6), 509–515.
Li, Z. W., Zhang, G. H., Geng, R., Wang, H. & Zhang, X. C. 2015 Land use impacts on soil detachment capacity by overland flow in the Loess Plateau, China. *Catena* **124**, 9–17.
Liu, B. Y., Nearing, M. A., Shi, P. J. & Jia, Z. S. 2000 Slope length relationships for soil erosion loss for steep slopes. *Soil Sci. Soc. Am. J.* **64** (5), 1759–1763.
Liu, Y., Yang, W., Yu, Z., Lung, I. & Gharabaghi, B. 2015 Estimating sediment yield from upland and channel erosion at a watershed scale using SWAT. *Water Resour. Manage.* **29** (5), 1399–1412.
Liu, F., Zhang, G. H., Sun, L. & Wang, H. 2016 Effects of biological soil crusts on soil detachment process by overland flow in the Loess Plateau of China. *Earth Surf. Process. Landf.* **41** (7), 875–883.
Lyle, W. M. & Smerdon, E. T. 1965 Relation of compaction and other soil properties to erosion resistance of soils. *Trans. ASAE* **8** (3), 419–422.
Mamo, M. & Bubenzer, G. D. 2001 Detachment rate, soil erodibility, and soil strength as influenced by living plant roots part II: field study. *Trans. ASAE* **44** (5), 1175–1181.
Merten, G. H., Nearing, M. A. & Borges, A. L. O. 2001 Effect of sediment load on soil detachment and deposition in rills. *Soil Sci. Soc. Am. J.* **65** (3), 861–868.

Meyer, L. D. & Wischmeier, W. H. 1969 Mathematical simulation of the processes of soil erosion by water. *Trans. ASAE* **12**, 754–758.

Misra, R. K. & Rose, C. W. 1996 Application and sensitivity analysis of process-based erosion model GUEST. *Eur. J. Soil Sci.* **47** (4), 593–604.

Morgan, R. P. C., Quinton, J. N., Smith, R. E., Govers, G., Poesen, J. W. A., Auerswald, K., Chisci, G., Torri, D. & Styczen, M. E. 1998 The European Soil Erosion Model (EUROSEM): a dynamic approach for predicting sediment transport from fields and small catchments. *Earth Surf. Process. Landf.* **23** (6), 527–544.

Nash, J. E. & Sutcliffe, J. V. 1970 River flow forecasting through conceptual models: part I. A discussion of principles. *Hydrology* **10** (3), 282–290.

Nearing, M. A. 1997 The mechanics of soil detachment by raindrops and runoff. *Eurasian Soil Sci* **30** (5), 552–556.

Nearing, M. A., Foster, G. R., Lane, I. J. & Finker, S. C. 1989 A process-based soil erosion model for USDA-water erosion prediction project technology. *Trans. ASAE* **32** (5), 1587–1593.

Nearing, M. A., Bradford, J. M. & Parker, S. C. 1991 Soil detachment by shallow flow at low slopes. *Soil Sci. Soc. Am. J.* **55** (2), 339–344.

Nearing, M. A., Norton, L. D., Bulgakov, D. A., Larionov, G. A., West, L. T. & Dontsova, K. M. 1997 Hydraulics and erosion in eroding rills. *Water Resour. Res.* **33** (4), 865–876.

Nearing, M. A., Simanton, J. R., Norton, L. D., Bulygin, S. J. & Stone, J. 1999 Soil erosion by surface water flow on a stony, semiarid hillslope. *Earth Surf. Process. Landf.* **24** (8), 677–686.

Nord, G. & Esteves, M. 2007 Evaluation of sediment transport formulae and detachment parameters in eroding rills using PSEM_2D and the Water Erosion Prediction Project (WEPP) database. *Water Resour. Res.* **43** (8), 2539–3545.

Shen, N., Wang, Z. L., Zhang, Q. W., Wu, B., Wang, D. D., Zhang, Q. L. & Liu, J. 2017 Quantifying the contribution of sediment load to soil detachment rate by sediment-laden rill flow. *Soil Sci. Soc. Am. J.* **81** (6), 1526–1536.

Su, Z. L., Zhang, G. H., Yi, T. & Liu, F. 2014 Soil detachment capacity by overland flow for soils of the Beijing region. *Soil Sci.* **179** (9), 446–453.

Thompson, J., Sattar, A., Gharabaghi, B. & Warner, R. 2016 Event-based total suspended sediment particle size distribution model. *J. Hydrol.* **536**, 236–246.

Trenouth, W. & Gharabaghi, B. 2015 Event-based soil loss models for construction sites. *J. Hydrol.* **524**, 780–788.

Wang, J. G., Li, Z. X., Cai, C. F., Yang, W., Ma, R. M. & Zhang, G. B. 2012 Predicting physical equations of soil detachment by simulated concentrated flow in Ultisols (subtropical China). *Earth Surf. Process. Landf.* **37** (6), 633–641.

Wang, D. D., Wang, Z. L., Shen, N. & Chen, H. 2016 Modeling soil detachment capacity by rill flow using hydraulic parameters. *J. Hydrol.* **535**, 473–479.

Xiao, H., Liu, G., Liu, P. L., Zheng, F. L., Zhang, J. Q. & Hu, F. N. 2017 Response of soil detachment rate to the hydraulic parameters of concentrated flow on steep loessial slopes on the Loess Plateau of China. *Hydrol. Process.* **31** (14), 2613–2621.

Yang, C. T. 1972 Unit stream power and sediment transport. *J. Hydraul. Div.* **98**, 1805–1826.

Zartl, A. S., Klik, A. & Huang, C. 2001 Soil detachment and transport processes from interrill and rill areas. *Phys. Chem. Earth B Hydrol. Oceans Atmos.* **26** (1), 25–26.

Zhang, G. H., Liu, B. Y., Nearing, M. A., Huang, C. H. & Zhang, K. L. 2002 Soil detachment by shallow flow. *Trans. ASAE* **45** (2), 351–357.

Zhang, G. H., Liu, B. Y., Liu, G. B., He, X. W. & Nearing, M. A. 2003 Detachment of undisturbed soil by shallow flow. *Soil Sci. Soc. Am. J.* **67** (3), 713–719.

Zhang, G. H., Liu, G. B., Tang, K. M. & Zhang, X. C. 2008 Flow detachment of soils under different land uses in the Loess Plateau of China. *Trans. ASABE* **51** (3), 883–890.

Zhang, G. H., Liu, Y. M., Han, Y. F. & Zhang, X. C. 2009a Sediment transport and soil detachment on steep slopes: I. Transport capacity estimation. *Soil Sci. Soc. Am. J.* **73** (4), 1291–1297.

Zhang, G. H., Liu, Y. M., Han, Y. F. & Zhang, X. C. 2009b Sediment transport and soil detachment on steep slopes: II. Sediment feedback relationship. *Soil Sci. Soc. Am. J.* **73** (4), 1298–1304.

First received 6 March 2018; accepted in revised form 3 August 2018. Available online 23 August 2018